DOI: 10.61782/fa.2023.1306

forum acusticum 2023

SIMULATION PROCEDURE TO DETERMINE IMPACT FORCE EXCITATION GENERATED BY AN ISO TAPPING MACHINE ON A WOODEN SLAB

Jesse Lietzén* **Juho Sormunen** **Sami Pajunen**
Mikko Kylliäinen
Tampere University, Unit of Civil Engineering, Finland

ABSTRACT

ISO standard tapping machine is a conventional and widely used standard impact sound source. Since the apparatus freely drops its hammers on the floor, the force level it produces depends on the type of the floor. Thus, to achieve accurate results with the impact sound insulation prediction models, the impact force excitation must be considered particularly in case of wooden floors. This study presents a simulation procedure to determine the impact force excitation generated by an ISO tapping machine. The applied methods comprise use of finite element method (FEM) and explicit time integration as well as a post-processing procedure. To demonstrate the applicability of the method, the finite element model was validated and applied to imitate an experimental situation on a cross-laminated timber (CLT) slab. The model validation showed that the computational model closely predicts the force pulse generated on the CLT slab. Findings from a sensitivity analysis revealed that local properties of the slab were the most important to the simulated impact force pulse. The findings are helpful for those developing simulation tools to compute the impact sound insulation of wooden floors.

Keywords: *impact sound insulation, impact force excitation, tapping machine, finite element method.*

**Corresponding author*: jesse.lietzen@tuni.fi.

1. INTRODUCTION

ISO standard tapping machine (STM) is probably the most widely used standard impact sound source applied in impact sound insulation measurements. The requirements for the STM have been given by the standards ISO 10140-5 [1] and ISO 16283-2 [2]. Although alternative impact sound sources have been presented, in many countries, the ISO tapping machine is used in the impact sound insulation measurements of all kinds of floors [3-4].

Since the STM freely drops its hammers on the floor, the force level it produces depends on the type of the floor [5], [6]. This is an essential feature that must be considered especially when wooden floors are studied. For example, the magnitude of the force spectrum generated by the STM is rather constant on bare concrete slabs whereas on wooden floors the spectrum depends on the floor configuration [7]. Theoretically, even the low-frequency level spectrum produced by the STM has a range of 6 dB, and the range rapidly expands with the increasing frequency [5].

To achieve accurate results with the impact sound insulation prediction models, the impact force excitation must be described paying a special attention when assessing wooden floors. Up to a certain extent, this can be done by applying the analytical models presented in the literature. In case of wooden floors, general models describing the interaction between the STM and the floor have previously been presented by Amiryarahmadi et al. [8], Brunskog and Hammer [5], Coguenanff et al. [9], Rabold et al. [10], and Wittstock [11].

In the recent decades, the use of the finite element method (FEM) to compute impact sound insulation of wooden floors has raised interests [12-16]. Thus, an appealing procedure would be to compute the impact force excitation by using a FEM tool. This also has several benefits in comparison with application of the analytical models [17].

The purpose of this paper is to present one possibility to solve the impact force excitation generated by the STM with the FEM tools. For this, we applied FEM and explicit time integration (i.e., explicit dynamics analysis) – techniques used in the field of computational impact mechanics. To demonstrate the performance and applicability of the presented simulation and post-processing procedures, we validated and applied the model to imitate an experimental situation on a cross-laminated timber (CLT) slab. To find out more about the study, see ref. [17].

2. MATERIALS AND METHODS

2.1 Procedure to determine the impact force excitation

STM exerts an array of force pulses by repeatedly dropping its five hammers to the floor. When neglecting a transient process of the change in individual force pulses (as described, e.g., by ref. [10]), this array of force pulses F_R can be determined for hammer α (1,2…5) in time and frequency domains as follows:

$$F_{R\alpha}(t) = \sum_{n=-\infty}^{\infty} F_{\alpha}(t - nT_r(1+k)) \quad (1)$$

$$F_{R\alpha}(f) = \sum_{n=-\infty}^{\infty} F_{n\alpha}\delta(f - nf_r) \quad (2)$$

where $F_\alpha(t)$ is the (constant) force pulse, k is a constant value depending on the order of the hammer fall, $F_{n\alpha}$ is the amplitude of discrete frequency components, $f_r = 1/T_r$ is the repetition rate for a single hammer, and $\delta(\cdot)$ denotes the Dirac delta function [5, 11]. With the order 1 – 3 – 5 – 2 – 4, k gets values [11]:

$$k = \begin{cases} 0, & if\ \alpha = 1 \\ 1/5, & if\ \alpha = 3 \\ 2/5, & if\ \alpha = 5 \\ 3/5, & if\ \alpha = 2 \\ 4/5, & if\ \alpha = 4 \end{cases} \quad (3)$$

Again, the (two-sided) amplitude spectrum for a force pulse can be evaluated with a Fourier transform [5]:

$$F_{n\alpha} = \frac{1}{T_r}\int_0^{T_r} F_{\alpha}(t - nT_r(1+k))e^{-2\pi nt/T_r}dt \quad (4)$$

Based on Eqns. (1–4) it is evident that the only unknown to determine the array of force pulses is the single force pulse $F_\alpha(t)$. In this paper, we focus on presenting FEM-models where the force pulses are simulated by applying explicit dynamics analysis (see Section 2.3). The abovementioned equations can be regarded as a post-processing procedure to achieve excitation data for time and frequency domain simulations, as illustrated by Fig. 1 [17].

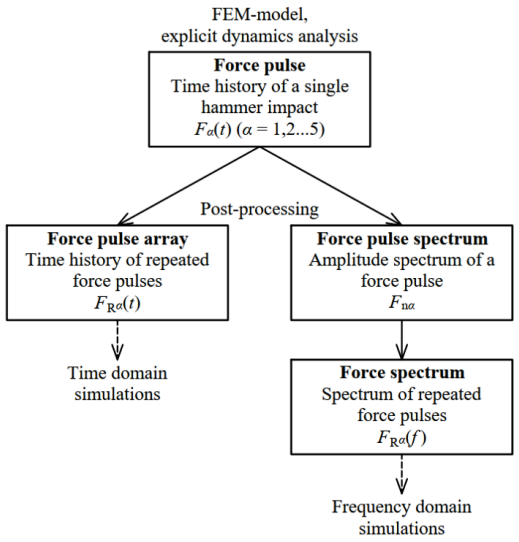

Figure 1. Procedure to determine the impact force excitation generated by the STM.

2.2 Experiments

The FEM-simulation results were compared with the experimental results [7, 17] on a 100 mm thick prefabricated cross-laminated timber (CLT) slab made of spruce [18] (Fig. 2). The slab was 3-layered and had lamellae of thicknesses 30, 40, and 20 mm. The boards of the slab (mostly of heartwood) were glued together only from their broader sides and the narrow sides were unglued. The width of the boards in the outer lamellae was mainly 130 mm and in the center 145 mm. The size of the slab was 2.4 x 2.68 m^2 and the slab was supported from its ends.

Figure 2. Schematic cross-section of the studied 100 mm CLT slab.

The experiments on the slab were carried out with an instrumented STM [7]. A force sensor (Kistler type 9712B5000) in the modified center hammer together with the signal acquisition system was used to determine the impact force input into the slab during the normal operation of the apparatus. The hammer itself was modified to fulfil the requirements for the tapping machine presented in the standards [1,2] together with the attached sensors and additional parts. The forces driving the slab were calculated from the measurement signals when the STM lied in five different positions S1–S5 (Fig. 3). Locally, the distances of the source positions from the board edges varied between positions.

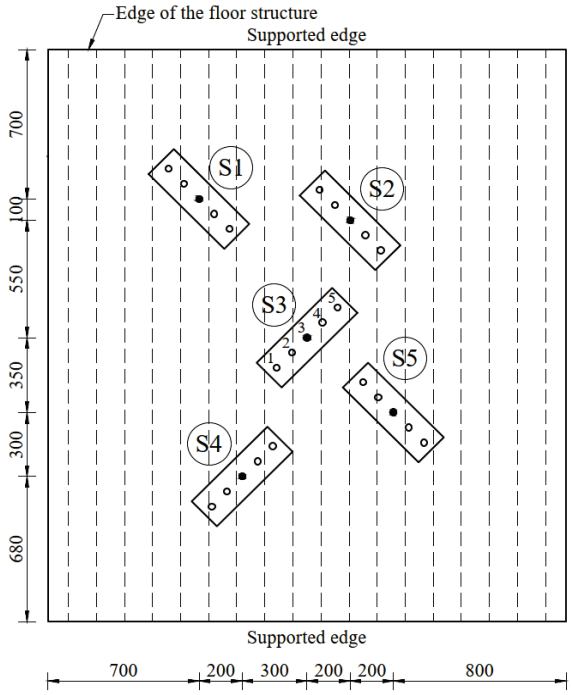

Figure 3. Source positions S1–S5.

2.3 Simulations

FEM Program Ansys LS-DYNA (smp s R10.1.0 Revision: 123264) was applied to simulate the impact force pulses generated by the STM on the CLT slab. The program applies explicit time integration to solve the dynamics of the system. The FEM model comprised of two colliding structural domains (hammer and slab) where the partial differential equation of motion governs in both domains:

$$\nabla \cdot \boldsymbol{\sigma} + \rho \boldsymbol{f} = \rho \ddot{\boldsymbol{x}} \tag{5}$$

where $\boldsymbol{\sigma}$ is the Cauchy stress tensor, ρ is density, $\boldsymbol{f}$ is body force density, and $\ddot{\boldsymbol{x}}$ is acceleration [19]. The contact between the bodies was considered frictional (μ = 0.5), and the contact was modelled by using a penalty method (LS-DYNA keyword: *CONTACT_AUTOMATIC_SINGLE_-SURFACE [20]). Thus, a regular contact-impact algorithm was used to simulate the collision between bodies. The model involved the curvature of the hammer head.

After a few mathematical operations, the finite element formulation of Eqn. (5) can be recognized as a matrix form of Newton's second law [19]. The central difference time integration method implemented in LS-DYNA [19] allows direct calculation of the nodal acceleration vector $\boldsymbol{a}$ on the basis of mass matrix **M** and force **F**:

$$\boldsymbol{a}^n = \mathbf{M}^{-1}\mathbf{F}^n \tag{5}$$

$$\boldsymbol{v}^{n+1/2} = \boldsymbol{v}^{n-1/2} + \boldsymbol{a}^n \Delta t^n \tag{6}$$

$$\boldsymbol{u}^{n+1} = \boldsymbol{u}^n + \boldsymbol{v}^{n+1/2} \Delta t^{n+1/2} \tag{7}$$

where $\boldsymbol{v}$ and $\boldsymbol{u}$ denote the nodal velocity and displacement vectors in time domain, respectively, and the time step Δt is:

$$\Delta t^{n+1/2} = (\Delta t^n + \Delta t^{n+1})/2 \tag{8}$$

The boards of the CLT slab were described as linear orthotropic elastic material with three principal directions being the longitudinal (L), radial (R), and tangential (T) axes with respect to the wood fiber direction. In the simulations, the parameters were (mostly) used to describe the materials in cartesian coordinate system. Values for all the parameters needed to capture the material behavior have not been presented by the standard EN 338 [21]. The remaining values were derived from the measurement results by Keunecke et al. [22] by scaling the results presented in their study with the standard values. Parameters used in the simulations for CLT have been shown in Table 1. The steel hammer was described with a linear elastic material model with density of 7641 kg/m^3, elastic modulus 205 000 MPa, and Poisson's ratio 0.3.

The simulated contact force pulses were filtered with a Butterworth filter of which cut-off frequency was 6000 Hz. Afterwards, a two-sided amplitude spectrum of the force F_n was determined. Furthermore, mechanical impulse I, low-frequency force F_{lf}, peak value of the force F_{peak} and the length of the pulse T_{pulse} were calculated to present the results in scalar values.

Table 1. Material parameters used to describe the orthotropic elastic behavior of spruce in strength class C24.

Material parameter	*C24*
Density ρ	**420 kg/m^3**
Elastic modulus E_L	**11 000 MPa**
Elastic modulus E_R	537 MPa
Elastic modulus E_T	**370 MPa**
Poisson's ratio ν_{LR}	0.36
Poisson's ratio ν_{LT}	0.45
Poisson's ratio ν_{TR}	0.21
Shear modulus G_{LR}	725 MPa
Shear modulus G_{LT}	**690 MPa**
Shear modulus G_{TR}	62 MPa

3. RESULTS AND DISCUSSION

3.1 Validation results

To ensure the validity of the element mesh, a mesh convergence study was carried out [17]. According to the study, the chosen mesh was constructed from elements of average length 2.5 mm near the impact area in the horizontal direction, and elsewhere the mesh was coarser (Fig. 4). In vertical direction, the CLT lamellae were formed from six, five, and four element layers, from top to bottom. An example of the kinetic energy transfer into the slab due to the collision has been shown in Fig. 5 using the chosen computational mesh. The change in the kinetic energy before and after the contact represents energy dissipation during the collision.

Figs. 6 and 7 illustrate the comparison of the simulated and measured force pulses in time and frequency domains, respectively. For brevity, the comparison has been shown for the results presenting simulations at two local extremes of the source positions: the position S2 lied 5 mm from the adjacent timber board and the position S3 was in the middle of board. To present the results for all the source positions, comparison of the simulated and measured pulses as the scalar values is available in Table 2.

The simulation and measurement results indicated reasonable equivalency (see Figs. 6 and 7, and Table 2). Hence, the computational model was regarded valid. However, differences between the simulation and measurement results in both force pulses and the force spectra are prominent. For example, the lengths of the simulated force pulses were shorter than the measured values at all the source positions. This can be explained with the low time resolution of the measurements in comparison with the simulations [7]. The magnitude spectra of the simulation results resembled the measured spectra closely but minor differences were prominent at frequencies above 2000 Hz. In the low-frequency range, discrepancies between the measured and simulated F_{lf} results correspond with not more than 0.7 dB level difference. The discrepancies are due to the differences between the energy dissipation during the collision and can also be seen from the differing impulse values.

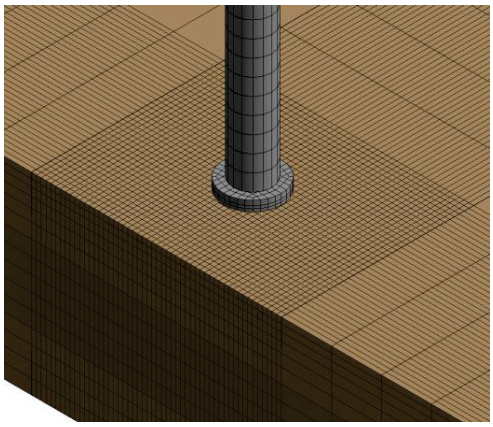

Figure 4. Horizontal and vertical element mesh of the hammer and the slab near the impact area.

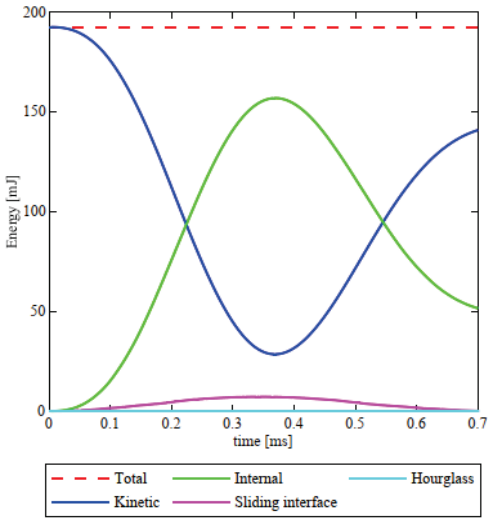

Figure 5. An example of the energy balance in the simulations (source position S3).

It was noticeable that the computational model led to minor spatial variation in comparison with the measurement results but local differences were prominent. For example, the highest simulated (as well

as measured) peak values of the force F_{peak} were received at the positions S3, and S5 which lied near the center of the boards (see Fig. 3). The lowest values were reached at the position S2 instead. This behaviour suggests that the local properties of the CLT slab affect the impact force. This can also be seen by illustrating the deformation during the collision (Fig. 8).

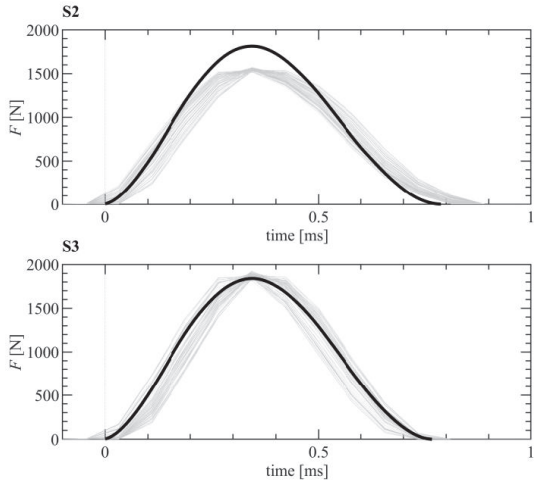

Figure 6. Simulated force pulses $F(t)$ at the source positions S2 and S3 (black lines) and the corresponding measurement results of individual pulses (grey lines) [7].

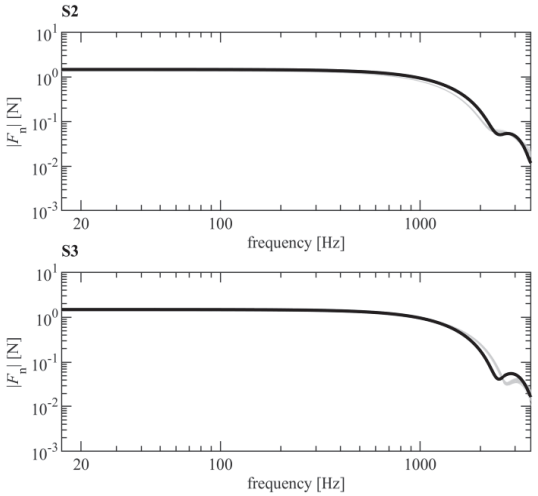

Figure 7. Simulated magnitudes of the two-sided amplitude spectra F_n at the source positions S2 and S3 (black lines) and the corresponding average measurement results (grey lines) [7].

Table 2. Scalar values for the measured (M) and simulated (S) force pulses at positions S1–S5.

Pos.	M/S	F_{peak} [N]	F_{lf} [N]	I [Ns]	T_{pulse} [ms]
S1	M	1662.5	1.42	0.71	0.99
	S	1833.4	1.48	0.74	0.77
S2	M	1546.3	1.36	0.68	1.02
	S	1813.3	1.47	0.74	0.79
S3	M	1878.5	1.40	0.70	0.91
	S	1839.3	1.48	0.74	0.77
S4	M	1699.4	1.47	0.74	1.01
	S	1822.2	1.48	0.74	0.78
S5	M	1832.8	1.45	0.73	0.94
	S	1838.2	1.48	0.74	0.77

3.2 Sensitivity analysis

The effect of the local and global properties to the impact force and reasons causing the differences between the measurement results at different source positions were studied with a sensitivity analysis. According to the analysis, it was evident that the global properties of the slab did not affect the simulation results of a single impact force pulse. For example, ignoring the gaps between the CLT boards and decreasing the size of the slab did not significantly decrease the accuracy of the simulations but their effect on the impact force were minor. Because of this, the sensitivity analysis was carried out with a slab having size 1000 mm x 1000 mm. Additionally, the model was found to be insensitive to the contact friction. [17]

Due to the abovementioned observations, the effect of local properties on the results was studied with three analyses. First, the local effects in the sectional direction of the CLT slab were studied (Fig. 9). This was performed by varying the strength class of the center lamella of the slab from C24 to C16 and C30 while keeping the outer lamellae as C24, as well as by introducing an imaginary material X10 with tenfold elastic and shear moduli to different slab layers. Secondly, the effect of the material parameters on the impact force was studied by varying all the material parameters a single parameter at a time (Fig. 10). An exception of this were the Poisson's ratios which were varied simultaneously. The range of the material parameters corresponded to the change in the strength class from C16 to C30. Third, since the CLT slab in the measurements was mainly made from heartwood, the effect of heartwood and sapwood (see Fig. 11) on the impact force was studied (Fig. 12). This was performed by solving the impact force presenting the material of the upmost lamella in different locally rotated cartesian coordinate systems A–D. [17]

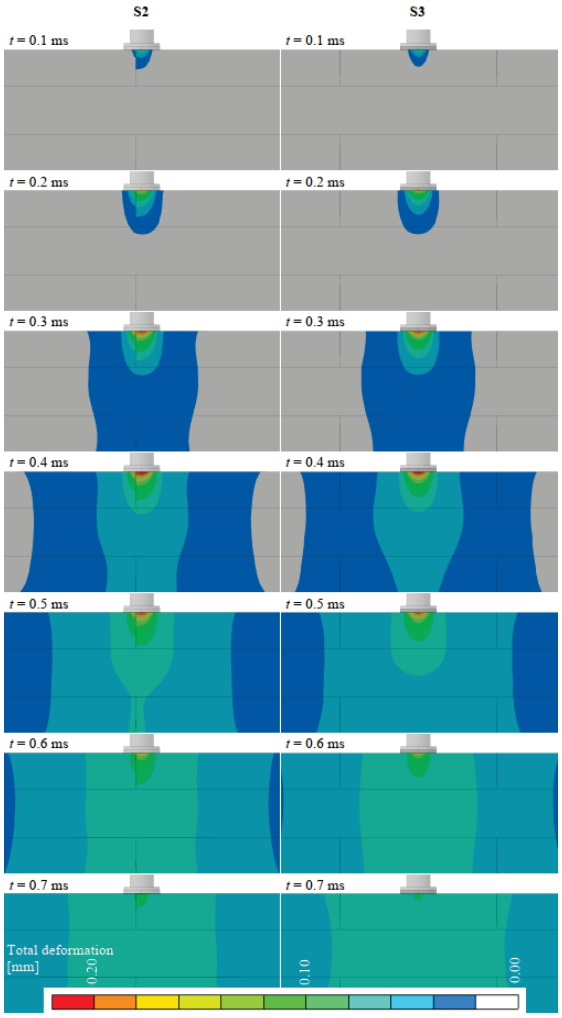

Figure 8. Total (elastic) deformation process during the impact at the source positions S2 and S3.

According to the results of the sensitivity analysis, the strength class of the center lamella has a minor effect on the impact force, but drastic changes in the stiffness properties can have a major effect on the force especially if the upper lamellae changes (c.f. tree knots) (Fig. 9). The results also show that the modulus of elasticity E_R, the shear modulus G_{LR}, and the density ρ have the greatest effect on the impact force (Fig. 10). Furthermore, the results clearly indicate that the spatial differences in the measurement results can be explained with the presence of heartwood in the CLT slab (Fig. 12). Hence, if the annual rings of wood are evident and the specimen is well known, the use of rotated cartesian (or cylindrical) coordinate system is justified for improving the computational accuracy.

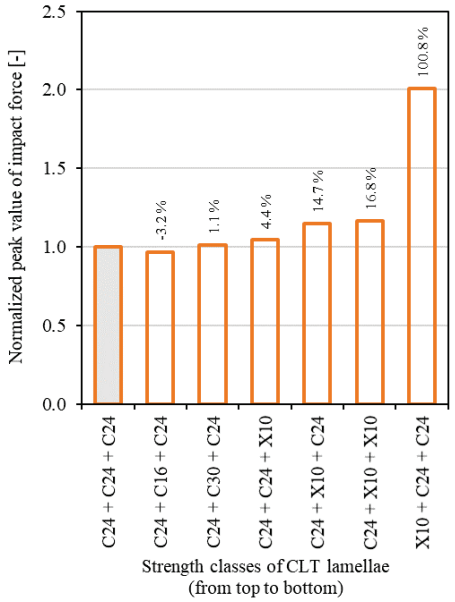

Figure 9. Sensitivity of the lamellae's strength class on the impact force (normalized to the result in grey).

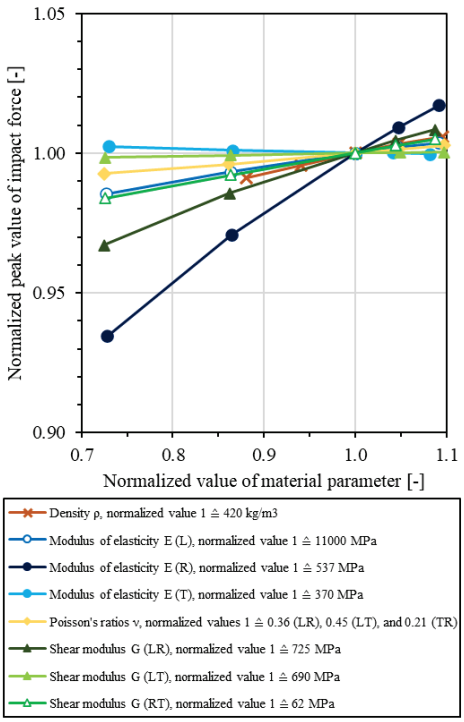

Figure 10. Sensitivity of material parameters of the CLT slab on the impact force.

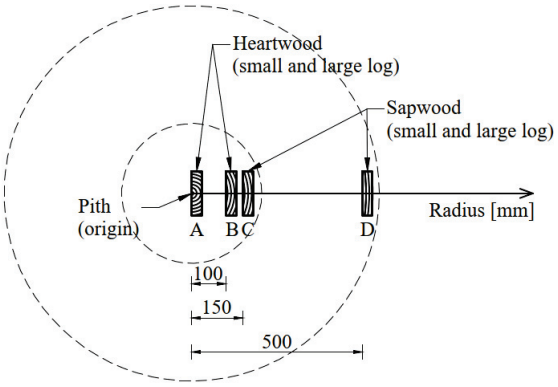

Figure 11. Locally rotated coordinate systems.

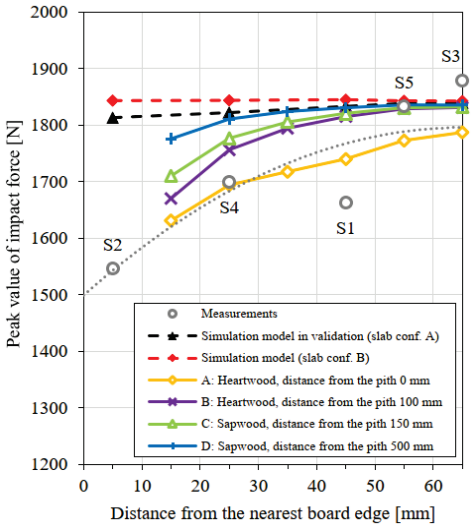

Figure 12. Effect of the heartwood and sapwood on the impact force. The average measurement results at different source positions have been indicated with labels S1–S5 and with a polynomial trend line of order two (dotted (:) grey line).

The results of the sensitivity analysis imply possibilities to develop the computational model further. The global effects, such as the size of the slab, had only a minor effect on the impact force. Thus, it is possible to predict the impact force pulse modelling the floor only partially. Additionally, in case of the CLT slab, results on the safe side can be reached by modelling the lamellae as continuous layers in a cartesian coordinate system. However, changes in material properties affect the results and lead to spatial variation even on CLT slabs. To consider this, the slab should be modelled in detail and using the best possible information from the material properties.

4. CONCLUSIONS

This paper presented a procedure to compute the impact force pulse generated by a hammer of the STM by using explicit dynamics analysis. The paper focuses on the computational model, but with the described post-processing method point forces describing the array of force pulses can be determined for time and frequency domain analyses. The validation of the FEM model showed that the analysis is applicable in predicting the impact force pulse on a wooden slab. The results in time and frequency domains were close to the maximum impact force measured on the CLT slab. Local properties of the CLT slab were discovered to be important to the results and explaining the discrepancies between the simulation and the measurement results. On the other hand, the global properties such as the location of the hammer on the slab and the slab size were found to be insignificant to the simulated impact force pulses. The findings from the sensitivity analysis offer possibilities to develop tools predicting the excitation force for both engineering and research purposes. The simulations were performed for a CLT slab, but the authors see no reason to restrict the use of the presented techniques to CLT or other massive wooden slabs only. Hence, the model can be applied on other types of wooden floors including surface structures such as additional layers, floating floors, or floor coverings, as well.

REFERENCES

[1] ISO 10140-5, Acoustics – Laboratory measurement of sound insulation of building elements – Part 5: Requirements for test facilities and equipment. Geneva: International Organization for Standardization, 2021.

[2] ISO 16283-2, Acoustics – Field measurement of sound insulation in buildings and of building elements – Part 2: Impact sound insulation. Geneve: International Organization for Standardization, 2015.

[3] B. Rasmussen, "Sound insulation between dwellings - Comparison of national requirements in Europe and interaction with acoustic classification schemes," in *Proc. of the International Congress on Acoustics*, (Aachen, Germany), pp. 5102–5109, 2019.

[4] M. Machimbarrena, B. Rasmussen, and C. Alves Monteiro, "Regulatory sound insulation requirements in South America – Status for housing, schools, hospitals and office buildings," in *Proc. of the Inter-Noise*, (Madrid, Spain), 2019.
[5] J. Brunskog and P. Hammer, "The interaction between the ISO tapping machine and lightweight floors," *Acta Acustica united with Acustica*, vol. 89, no. 2, pp. 296–308, 2003.
[6] L. Cremer, M. Heckl, and B. A. T. Petersson: *Structure-Borne Sound*. Berlin Heidelberg: Springer-Verlag, 2005.
[7] J. Lietzén, J. Miettinen, M. Kylliäinen, and S. Pajunen, "Impact force excitation generated by an ISO tapping machine on wooden floors," *Applied Acoustics*, vol. 175, 107821, 2021.
[8] N. Amiryarahmadi, W. Kropp, D. Bard, and K. Larsson, "Time-domain model of a tapping machine," in *Proc. of Forum Acusticum*, (Aalborg, Denmark), pp. 1713–1718, 2011.
[9] C. Coguenanff, C. Guigou-Carter, P. Jean, and C. Desceliers, "Probabilistic model of the impact force spectrum for the standard ISO tapping machine," in *Proc. of the 22nd International Congress on Sound and Vibration ICSV*, (Florence, Italy), pp. 5551–5558, 2015.
[10] A. Rabold, M. Buchschmid, A. Düster, G. Müller, and E. Rank, "Modelling the excitation force of a standard tapping machine on lightweight floor structures," *Building Acoustics*, vol. 17, no. 3, pp. 175–197, 2010.
[11] V. Wittstock, "On the spectral shape of the sound generated by standard tapping machines," *Acta Acustica united with Acustica*, vol. 98, no. 2, pp. 301–308, 2012.
[12] A. Rabold, A. Düster, and E. Rank, "FEM based prediction model for the impact sound level of floors," in *Proc. of the Meetings in Acoustics*, (Paris, France), pp. 2993–2998, 2008.
[13] M. Kohrmann, M. Buchschmid, U. Schanda, and G. Müller, "A FEM-based planning tool for the vibro-acoustic design of wooden floors at low frequencies," in *Proc. of the Inter-Noise*, (Hamburg, Germany), pp. 3743–3751, 2016.
[14] D. Bard et al., "Modelling prerequisites – FEM/SEA Impact and Airborne Sound. Silent Timber Build, report no STB01 WG1," RISE Research Institutes of Sweden AB, 2017.
[15] C. Qian, S. Ménard, D. Bard-Hagberg, J. L. Kouyoumji, and J. Negreira, "Calibration of the ISO tapping machine for finite-element prediction tool on a wooden-base floor," *Building Acoustics*, vol. 26, no. 3, pp. 157–167, 2019.
[16] P. Wang, C. Van hoorickx, G. Lombaert, and E. Reynders, "Numerical prediction and experimental validation of impact sound radiation by timber joist floors," *Applied Acoustics*, vol. 162, p. 107182, 2020.
[17] J. Lietzén, J. Sormunen, S. Pajunen, and M. Kylliäinen, "Simulation of impact force generated by an ISO tapping machine on a wooden slab using explicit dynamics analysis," *Engineering Structures*, vol. 270, 114855, 2022.
[18] ETA-14/0349, "European Technical Assessment," Austrian Institute of Construction Engineering. 2014.
[19] LS-DYNA Theory Manual (r:8571). Livermore, California: Livermore Software Technology Corporation (LSTC), 2017.
[20] LS-DYNA Keyword User's Manual, Volume I (r:8752). Livermore, California: Livermore Software Technology Corporation (LSTC); 2017.
[21] EN 338, Structural timber – Strength classes. Brussels, 2016.
[22] D. Keunecke, S. Hering, and P. Niemz, "Three-dimensional elastic behaviour of common yew and Norway spruce," *Wood Science and Technology*, vol. 42, no. 8, pp. 633–647, 2008.